Analysis of Varactor Frequency Multipliers: Nonlinear Behavior and Hysteresis Phenomena

ELIO BAVA, GIAN PAOLO BAVA, ALDO GODONE, AND GIOVANNI RIETTO

Abstract—**A nonlinear analysis of varactor frequency multipliers has been performed and numerically implemented to obtain the quantities that must be specified to define the quality of a multiplier used to generate high spectral purity signals for metrological purposes.**

The theoretical model has proved adequate to predict the existence of complicated hysteresis phenomena, confirmed by experimental investigation.

The practical cases examined refer to abrupt-junction doublers and triplers operating in self-bias conditions. The circuit parameters have been determined for maximum efficiency at a given generator available power. Then, some effects of input power, frequency, and tuning variations have been investigated, and calculated curves including hysteresis cycles are shown.

Beside the optimization of the multiplier operation, the equations given are sufficiently general to yield the information requested on multipliers of this kind, where the power handling capabilities of the varactor are not fully exploited but the high spectral purity of the input signals must be preserved. As an example, one of the most important features of the frequency multiplier, i.e., the AM–PM conversion, was determined in a practical case for varying input power levels.

I. Introduction

THE SYNTHESIS of high spectral purity signals in the microwave and far-infrared regions requires strict specifications for frequency multipliers. Besides a high efficiency, very good performance is necessary as regards the additive noise and the input–output (I/O) transfer characteristics for the amplitude and phase fluctuations.

These requirements are particularly important in view of the present availability of master oscillators with outstanding performance, e.g., power spectral densities of white phase noise of 10^{-18} rad^2·Hz^{-1}. When the noise characteristics play a predominant role, as in frequency multiplication chains, the varactor multiplier shows very interesting features.

Some experimental determinations on AM–PM conversion in several frequency multipliers have been reported [1].

In this work, varactor frequency multipliers are theoretically analyzed, with special reference to nonlinear behavior and hysteresis phenomena, arising for available input power variations in a circuit whose efficiency has been maximized at a given power level. At the same time, the static AM–PM and AM–AM conversions are obtained. The calculations are carried out only for abrupt-junction doublers and triplers with self-bias.

Manuscript received June 10, 1977; revised January 3, 1978. This work was supported by the Italian National Research Council.

E. Bava, A. Godone, and G. Rietto are with the Istituto Elettrotecnico Nazionale Galileo Ferraris, Torino, Italy.

G. P. Bava is with the Istituto di Elettronica e Telecomunicazioni del Politecnico, Torino, Italy.

The transfer functions for amplitude and phase fluctuations and I/O conversions versus the Fourier angular frequency will be analyzed in a following paper.

II. Analysis of a Varactor Multiplier

The present paper considers varactor frequency multipliers with and without idler, operating in the "shunt diode" mode [2].

The equivalent circuit used is shown in Fig. 1. Subscripts "1," "i," and "out" refer to the three meshes indicated. The following assumptions are made.

1) The parasitic parameters of the varactor, in particular, its series resistance, are included in the impedances Z_n ($n=1$, i, out) (for the discussion of the varactor model see [2] and [3]).

2) The impedances Z_n have filtering characteristics so as to allow the current flow only in a narrow band around the resonance frequency.

3) The angular frequencies ω_{out} and ω_i are multiples of ω_1.

The second assumption allows expressing the charge q in the varactor as follows:

$$q = q_0 + Q_1 + Q_i + Q_{\text{out}} \tag{1}$$

where q_0 is the average value of the charge and

$$Q_n(t) = q_n(t) \sin\left[\omega_n t + \varphi_n(t)\right]. \tag{2}$$

$q_n(t)$ and $\varphi_n(t)$ are the amplitude and phase fluctuations of the charges and are supposed to be slowly varying time functions.

As regards the analysis of fluctuations, the impedances $Z_n(R_n + jX_n)$ are represented by a simple series-resonant circuit (R_n, L_n, C_n); more complex reactances are replaced with the equivalent series-resonator circuit near the angular frequency ω_n.

The voltage across Z_n is

$$\begin{aligned} V_n &= R_n I_n + L_n \frac{dI_n}{dt} + \frac{Q_n}{C_n} \\ &\cong \left[R_n\left(\omega_n + \frac{d\varphi_n}{dt}\right) q_n + 2\omega_n L_n \frac{dq_n}{dt} \right] \cos(\omega_n t + \varphi_n) \\ &\quad + \left(R_n \frac{dq_n}{dt} - X_n \omega_n q_n - 2\omega_n L_n q_n \frac{d\varphi_n}{dt} \right) \sin(\omega_n t + \varphi_n) \end{aligned} \tag{3}$$

having neglected the second derivatives and the products of first derivatives of q_n and φ_n; this approximation holds when $\Omega \ll 2\pi B$ where Ω is the Fourier angular frequency of fluctuations and $B = R_n/2\pi L_n$ is the bandwidth of the mesh at ω_n.

0018-9480/79/0200-0141$00.75

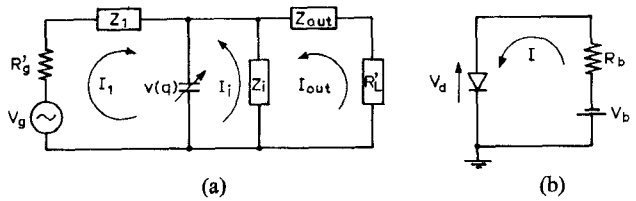

Fig. 1. (a) RF equivalent circuit of the multiplier. (b) Bias network. Varactor parasitic parameters included in Z_1, Z_i, Z_{out}.

The mesh equations for the circuit of Fig. 1, at the corresponding frequencies, are

$$V_g = R_g' I_1 + V_1 + v_1$$
$$0 = V_i + v_i$$
$$0 = R_L' I_{out} + V_{out} + v_{out}$$

where v_n is the voltage across the varactor at ω_n and $V_g = v_g(t) \cos [\omega_1 t + \varphi_g(t)]$.

Separating in-phase and quadrature components in the above equations [4], the following system is obtained:

$$v_g \cos(\varphi_1 - \varphi_g) = R_g\left(1 + \frac{1}{\omega_1}\frac{d\varphi_1}{dt}\right)\omega_1 q_1 + 2\omega_1 L_1 \frac{dq_1}{dt} + F_c^1$$

$$v_g \sin(\varphi_1 - \varphi_g) = R_g \frac{dq_1}{dt} - X_1 \omega_1 q_1 - 2\omega_1 L_1 q_1 \frac{d\varphi_1}{dt} + F_s^1$$

$$0 = R_L\left(1 + \frac{1}{\omega_{out}}\frac{d\varphi_{out}}{dt}\right)\omega_{out} q_{out} + 2\omega_{out} L_{out}\frac{dq_{out}}{dt} + F_c^{out}$$

$$0 = R_L \frac{dq_{out}}{dt} - X_{out}\omega_{out} q_{out} - 2\omega_{out} L_{out} q_{out}\frac{d\varphi_{out}}{dt} + F_s^{out}$$

$$0 = R_i\left(1 + \frac{1}{\omega_i}\frac{d\varphi_i}{dt}\right)\omega_i q_i + 2\omega_i L_i \frac{dq_i}{dt} + F_c^i$$

$$0 = R_i \frac{dq_i}{dt} - X_i \omega_i q_i - 2\omega_i L_i q_i \frac{d\varphi_i}{dt} + F_s^i \qquad (4)$$

where

$$R_g = R_g' + R_1$$
$$R_L = R_L' + R_{out}$$
$$F_c^n = \frac{\omega_1}{\pi}\int_{-\pi/\omega_1}^{+\pi/\omega_1} v(q) \cos(\omega_n t + \varphi_n)\, dt$$
$$F_s^n = \frac{\omega_1}{\pi}\int_{-\pi/\omega_1}^{+\pi/\omega_1} v(q) \sin(\omega_n t + \varphi_n)\, dt.$$

Here, in order to evaluate F_c^n and F_s^n, it is necessary to define the voltage-charge characteristic of the diode and the multiplication order, so as to neglect the terms at frequencies other than those under consideration.

In the present paper, the calculations are carried out for a doubler and a tripler with an abrupt-junction varactor having the following characteristic:

$$v(q) = V_0 - mq^2, \qquad m = \frac{1}{4V_0 C_0^2} \qquad (5)$$

where V_0 is the contact potential and C_0 is the zero-bias capacitance.

In this case, the expressions for a tripler (by putting subscripts $i=2$, out$=3$) are as follows:

$$F_c^1 = -mq_1 q_2 \cos(\varphi_2 - 2\varphi_1) - mq_2 q_3 \cos(\varphi_3 - \varphi_2 - \varphi_1)$$
$$F_s^1 = mq_1 q_2 \sin(\varphi_2 - 2\varphi_1) + mq_2 q_3 \sin(\varphi_3 - \varphi_2 - \varphi_1) - 2mq_0 q_1$$
$$F_c^2 = -mq_1 q_3 \cos(\varphi_3 - \varphi_2 - \varphi_1) + m\frac{q_1^2}{2}\cos(\varphi_2 - 2\varphi_1)$$
$$F_s^2 = mq_1 q_3 \sin(\varphi_3 - \varphi_2 - \varphi_1) + m\frac{q_1^2}{2}\sin(\varphi_2 - 2\varphi_1) - 2mq_0 q_2$$
$$F_c^3 = mq_1 q_2 \cos(\varphi_3 - \varphi_2 - \varphi_1)$$
$$F_s^3 = mq_1 q_2 \sin(\varphi_3 - \varphi_2 - \varphi_1) - 2mq_0 q_3. \qquad (6)$$

The doubler equations are obtained by neglecting the last two lines in both (4) and (6) and putting subscript out$=2$ and $q_3 = 0$.

Equation (4) will be used for studying the I/O transfer characteristics of fluctuations in a following paper. Here, only steady-state conditions will be considered.

III. Steady-State Operation

Design criteria for multipliers under different working conditions are extensively discussed in the literature [2], [3], [5]–[8]. The most frequently examined situations are the current drive and the maximum elastance variation (between breakdown and forward conduction). In the case of frequency multipliers for high spectral purity signals, the varactor capacitance range is not fully exploited for noise reasons. Therefore, a constant generator available power P_{av} is assumed in the following considerations.

In this section, relations (4) and (6) are rewritten for a doubler and a tripler under steady-state conditions, and the bias equations are introduced ((7)–(9)). From this set of equations, the maximum efficiency conditions can be derived. The main expressions and results regarding this derivation are reported in the Appendix.

However, the maximum efficiency criterion does not take into account other factors which may affect the multiplier performance. In our case, they are mainly: parasitic oscillations [8], [9], AM–PM conversion [1], [10], AM distortion, and hysteresis phenomena [2], [11]. Some of these effects will be considered in Section IV.

A. Doubler Case

From systems (4) and (6) modified for a doubler under steady-state conditions ($d/dt=0$), the following set of equations is obtained:

$$\begin{aligned} v_{g0}\cos(\varphi_{10}-\varphi_{g0}) &= \omega_1 q_{10}\left(R_g-\frac{mq_{20}\cos\varphi_0}{\omega_1}\right)\\ v_{g0}\sin(\varphi_{10}-\varphi_{g0}) &= -X_1\omega_1 q_{10}-2mq_0q_{10}\\ &\quad +mq_{10}q_{20}\sin\varphi_0\\ 0 &= R_L\omega_2 q_{20}+\frac{m}{2}q_{10}^2\cos\varphi_0\\ 0 &= -X_2\omega_2 q_{20}+\frac{m}{2}q_{10}^2\sin\varphi_0-2mq_0q_{20} \end{aligned} \tag{7}$$

where subscript "0" refers to the steady-state values and $\varphi_0=\varphi_{20}-2\varphi_{10}$, $\omega_2=2\omega_1$.

q_{10} and q_{20} will be assumed positive, which implies, taking into account the third equation above, $\cos\varphi_0<0$.

B. Tripler Case

By putting $i=2$, out$=3$, and $d/dt=0$ in (4) and (6), the following system for the steady-state operation of the tripler shown in Fig. 1 is obtained:

$$\begin{aligned} v_{g0}\cos(\varphi_{10}-\varphi_{g0}) &= \omega_1 q_{10}\left(R_g-\frac{mq_{20}\cos\varphi_0}{\omega_1}\right.\\ &\quad \left.-\frac{mq_{20}q_{30}\cos\psi_0}{\omega_1 q_{10}}\right)\\ v_{g0}\sin(\varphi_{10}-\varphi_{g0}) &= -X_1\omega_1 q_{10}+mq_{10}q_{20}\sin\varphi_0\\ &\quad +mq_{20}q_{30}\sin\psi_0-2mq_0q_{10}\\ 0 &= R_L\omega_3 q_{30}+mq_{10}q_{20}\cos\psi_0\\ 0 &= -X_3\omega_3 q_{30}+mq_{10}q_{20}\sin\psi_0-2mq_0q_{30}\\ 0 &= R_2\omega_2 q_{20}-mq_{10}q_{30}\cos\psi_0+\frac{m}{2}q_{10}^2\cos\varphi_0\\ 0 &= -X_2\omega_2 q_{20}+mq_{10}q_{30}\sin\psi_0\\ &\quad +\frac{m}{2}q_{10}^2\sin\varphi_0-2mq_0q_{20} \end{aligned} \tag{8}$$

where $\varphi_0=\varphi_{20}-2\varphi_{10}$, $\psi_0=\varphi_{30}-\varphi_{20}-\varphi_{10}$.

C. Bias

Considering the bias circuit (Fig. 1(b)), where V_d is the average voltage across the varactor and I is the detected current, the mesh equation is

$$-V_b-R_bI=V_d. \tag{9}$$

V_d is given directly by (5):

$$\begin{aligned} V_d &= V_0-m\langle q^2\rangle\\ &= V_0-m\left(q_0^2+\frac{q_{10}^2+q_{20}^2+q_{30}^2}{2}\right) \end{aligned}$$

and, in the case of a doubler, $q_{30}=0$.

I is derived from the voltage-current characteristic of the diode; therefore,

$$I=\frac{I_s}{2\pi}\int_0^{2\pi}(e^{v(q)/V_T}-1)\,d(\omega_1 t).$$

If we put $R_b=0$ in (9), q_0 is readily obtained:

$$q_0=-\sqrt{\frac{V_0+V_b}{m}-\frac{q_{10}^2+q_{20}^2+q_{30}^2}{2}} \tag{10}$$

corresponding to the fixed-bias case.

Usually, the most common technique is self-bias; in this case, $V_b=0$. In order to determine q_0, (9) must be solved numerically.

IV. Power, Frequency, and Tuning Variations

AM–PM conversion and hysteresis phenomena in frequency multipliers have been reported in the literature [1], [10], [11]. In this section, these aspects are theoretically examined with reference to the abrupt-junction multipliers previously analyzed.

For the numerical calculations, the following values of the circuit parameters are assumed: $m=6.67\times10^{20}$, $V_T=0.04$ V, $R_bI_s=0.1$ V, $R_1=R_2=R_3=2\ \Omega$, and the operating frequencies are $f_1=500$ MHz for the doubler and $f_1=300$ MHz for the tripler.

A. Available Power Variation

If the generator power is changed from the value assumed for the circuit design, the quantities of interest, in the doubler case, can be calculated by solving the system formed by (7) and (9), keeping R_g', R_L', X_1, and X_2 constant and determining (e.g., by iteration) the unknown values q_0, φ_0, $\varphi_{10}-\varphi_{g0}$, q_{10}, q_{20}, and V_d. In this case, the efficiency is given by the general expression (A1).

Figs. 2–4 show typical curves of V_d, φ_2 (for $\varphi_g=0$), and η, respectively, for varying P_{av}, using the values previously indicated for the different parameters.

An interesting hysteresis phenomenon can be noticed; from the analytical point of view, this is due to the N-shaped curve of I versus q_0, which can originate multiple intersections in solving (9).

In Fig. 3, the static AM–PM conversion of the doubler is reported. This parameter is particularly significant to define the output phase spectrum deterioration due to the input amplitude fluctuations. In the maximum efficiency zone, the conversion coefficient may reach values (e.g., 30°/dB) whose effect sometimes cannot be neglected as regards the spectral purity of the output signals [1].

From Fig. 4, the AM distortion of the doubler can also be obtained.

The presence and shape of the hysteresis cycle is little affected by R_bI_s, whereas it is extremely sensitive to the values of the reactances X_1 and X_2. A quantitative analysis of this last point has been performed with reference to the previous numerical example. Figs. 5 and 6 show the curves of the limiting P_{av} values for the hysteresis cycle, the efficiency, and the AM–PM conversion coefficient

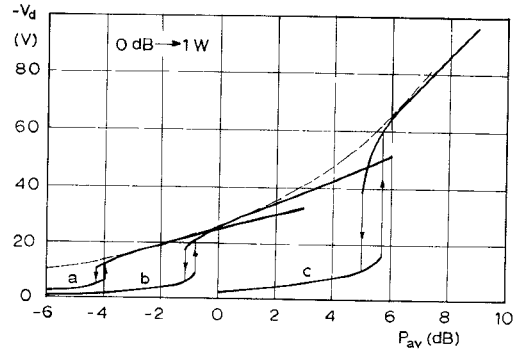

Fig. 2. Varactor doubler (0.5–1 GHz); self-bias voltage V_d versus generator available power P_{av}. Maximum efficiency power level: *a* 0.5 W, *b* 1 W, and *c* 4 W.

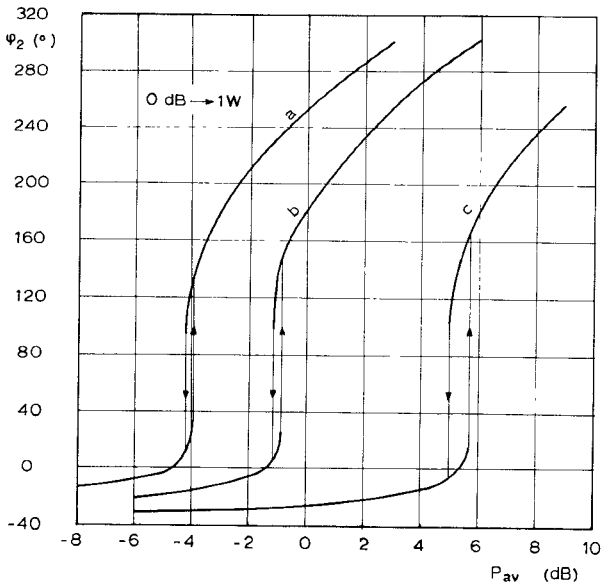

Fig. 3. Varactor doubler (0.5–1 GHz); output phase φ_2 ($\varphi_g = 0$) versus generator available power P_{av}. Maximum efficiency power level: *a* 0.5 W, *b* 1 W, and *c* 4 W.

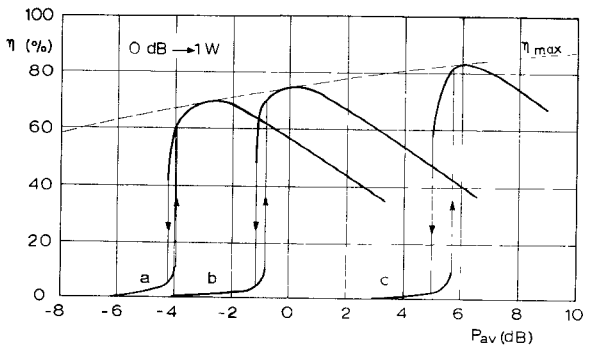

Fig. 4. Varactor doubler (0.5–1 GHz); efficiency η versus generator available power P_{av}. Maximum efficiency power level: *a* 0.5 W, *b* 1 W, and *c* 4 W.

versus X_1/X_{10} and X_2/X_{20}, respectively, corresponding to the 1-W nominal power. X_{10} and X_{20} are the reactance values for maximum efficiency (see Appendix).

Changing X_2 does not help to significantly reduce and shift the hysteresis cycle, not even at the expense of an important impairment of η. On the contrary, when X_1 is reduced, the hysteresis cycle shifts towards lower power levels, and, at the same time, its width decreases until it vanishes at $\eta = 0.585$, an efficiency impairment which is perfectly tolerable in frequency multipliers for high spectral purity signals.

It also appears that the AM–PM conversion coefficient is very sensitive to X_1 and X_2 variations, and, in particular, it increases very rapidly for growing X_1. Then, reducing X_1 is advantageous also from this point of view.

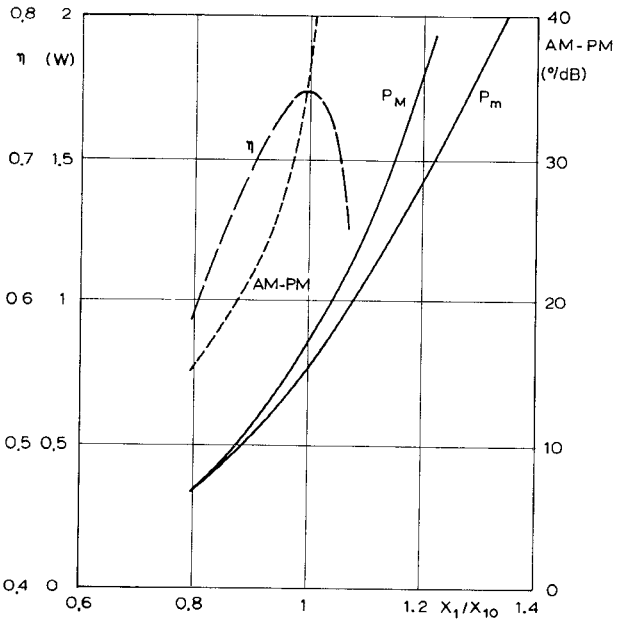

Fig. 5. Lower (P_m) and upper (P_M) limit of the hysteresis cycle, efficiency η, and AM–PM conversion coefficient versus X_1/X_{10}. Maximum efficiency power level 1 W.

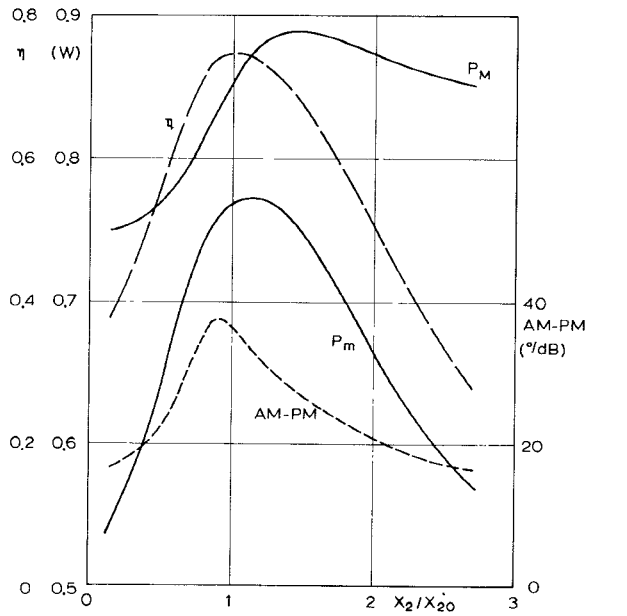

Fig. 6. Lower (P_m) and upper (P_M) limit of the hysteresis cycle, efficiency η, and AM–PM conversion coefficient versus X_2/X_{20}. Maximum efficiency power level 1 W.

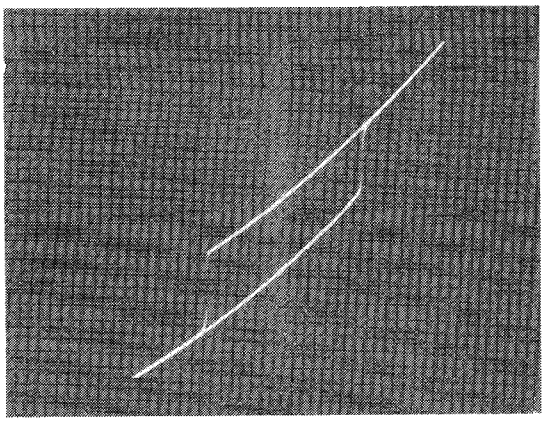

Fig. 7. Photograph of a typical hysteresis phenomenon in a doubler ($f_1 = 100$ MHz). Input amplitude level on the horizontal axis, diode voltage on the vertical axis.

A different approach for eliminating the hysteresis effects should be fixed bias, since, in this case, the N-shaped curve of the left hand side of (9) becomes a horizontal straight line.

No experimental investigation was systematically carried out. However, a doubler, using a BAY 66 varactor at $f_1 = 100$ MHz, was built and adjusted in order to visualize the above phenomena, which were all actually observed. A photograph displaying a typical hysteresis case is shown in Fig. 7. Parasitic oscillations were also noticed in some parts of the hysteresis cycle, originating modulation lines at ω_1 and ω_2. The theoretical analysis of these oscillations, though under different operating conditions, has been performed in papers [8], [9].

All the above mentioned effects obviously exist also in the tripler case, which can be examined by using (8) and (9). Here, again, interesting and complicated hysteresis phenomena arise. Figs. 8 and 9 show typical curves of the self-bias voltage, the output phase when $\varphi_g = 0$, and the efficiency for a tripler optimized at $P_{av} = 1$ W. The parameters are the same as indicated above with a definite choice for φ_0.

If the other value for φ_0 is chosen, since the tuning reactances are changed, important variations in the shape of the hysteresis cycle occur. Near the maximum-efficiency point, the AM–PM conversion in the example given appears to be of the order of 20°/dB.

Fig. 10 shows the photograph of a hysteresis cycle on V_d for a tripler from 100 to 300 MHz realized with a BAY 66 diode.

B. Input Frequency Variation

Some authors have analyzed the bandwidth characteristics of multipliers [11]–[13]. Here, hysteresis phenomena appearing in frequency responses are calculated for the abrupt-junction doubler discussed in the previous sections. The multiplier behavior is strongly influenced by the reactances X_1 and X_2. Once the dependence of X_1 and X_2 on frequency is established, (7), (9), and (A1) are used to determine the circuit response. With reference to the numerical example reported above, two cases have been

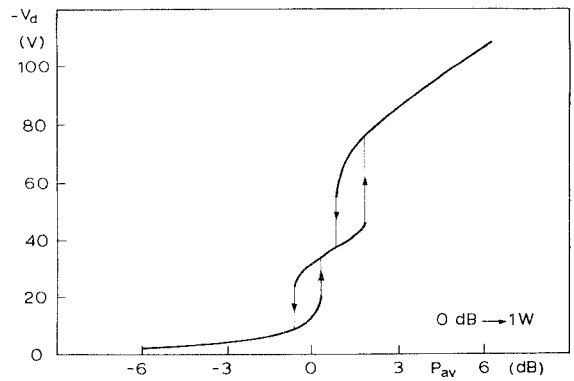

Fig. 8. Varactor tripler (300–900 MHz); self-bias voltage V_d for a circuit with maximum efficiency at 1 W.

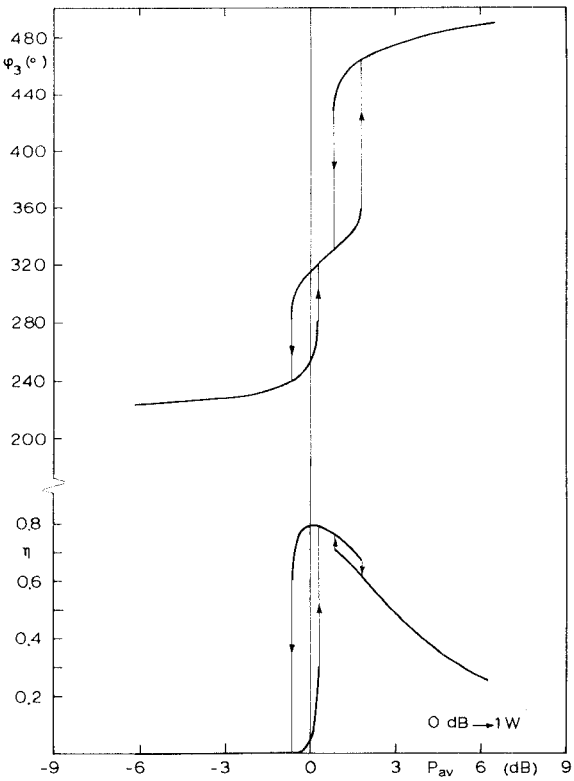

Fig. 9. Varactor tripler (300–900 MHz); output phase φ_3 and efficiency η for a circuit with maximum efficiency at 1 W.

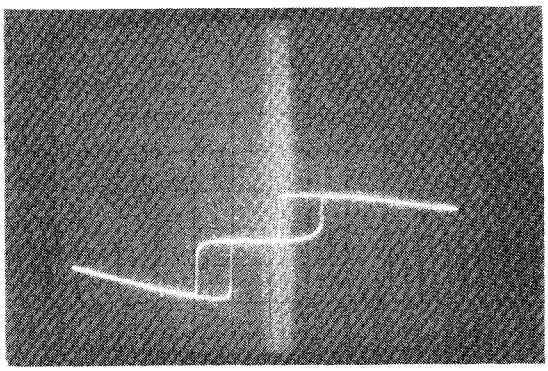

Fig. 10. Photograph of a typical hysteresis phenomenon in a tripler ($f_1 = 100$ MHz). Input amplitude level on the horizontal axis, diode voltage on the vertical axis.

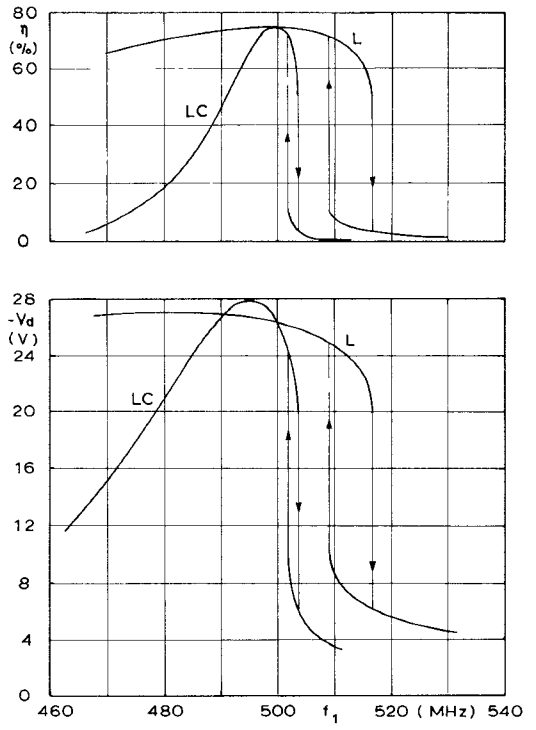

Fig. 11. Calculated frequency responses for efficiency η and self-bias voltage V_d in an abrupt-junction doubler. Input frequency $f_1 = 500$ MHz; L = input and output circuits consisting of simple inductances and LC = input and output circuits consisting of series resonators.

examined in detail: 1) X_n are simple inductances, and 2) X_n are series-resonant circuits.

In both cases, (A3) must be satisfied at the design frequency. This condition completely determines the inductance values in the first case, whereas, in the second case, the resonance frequencies of the input and output circuits were chosen to be 0.9 $\omega_1/2\pi$ and 0.95 $\omega_2/2\pi$, respectively, as an example.

The calculated efficiency and self-bias voltage curves are given in Fig. 11.

The shape of the curves, including the hysteresis cycle, shows a marked dependence on the choice of the input and output circuits.

V. Conclusions

An analytical model of the abrupt-junction varactor frequency multiplier has been developed in order to determine the conditions for maximum efficiency at a given generator available power. Self-bias operation is assumed.

The model has proved sufficiently general to yield the information requested on high spectral purity multipliers. In particular, it is possible to calculate the AM–PM conversion, which is one of the most important features of a frequency multiplier and, in certain circumstances, may reach significant values (e.g., 30°/dB for a doubler).

Some cases of operation under conditions different from the design values have been numerically evaluated. Calculated curves for varying input power or frequency show hysteresis phenomena which, in a practical example, have been experimentally verified.

The influence of tuning variations in the input and output circuits on the position and shape of the hysteresis cycle has been separately analyzed. It appears that a proper choice of the input circuit can eliminate power hysteresis with a tolerable impairment of efficiency, at the same time reducing the AM–PM conversion coefficient.

The equations (4), given at the beginning of this paper, are the starting point for the study of the transfer functions of the amplitude and phase fluctuations and of the additive noise. These topics will be discussed in a following paper.

VI. Appendix

The multiplier efficiency is

$$\eta = \frac{P_{out}}{P_{av}} = 4R_g' R_L' \left(\frac{\omega_{out} q_{out}}{v_{g0}} \right)^2. \tag{A1}$$

The maximum of η, for a given available power of the generator, is obtained with a proper choice of R_g' and R_L', that is suitable matching circuits, and of the tuning reactances X_1, X_2 (and X_3 for a tripler), or the angles $\varphi_{10} - \varphi_{g0}$ and φ_0 (ψ_0 for a tripler). This work is found in the literature (for instance, [2] for a doubler), and only the results needed are reported in this Appendix.

A. Doubler Case

The R_g', R_L', φ_0, X_{10}, X_{20} required for maximum efficiency are the solutions of the following equations:

$$\left(\frac{R_g'}{R_1} \right)^3 - \left(\frac{R_g'}{R_1} \right)^2 = \frac{m^2}{4\omega_1^4 R_1^2 R_2} P_{av} = k_2$$

$$\frac{R_L'}{R_2} = 2\frac{R_g'}{R_1} - 1$$

$$\varphi_0 = \pi \tag{A2}$$

$$X_{10} = -\frac{2mq_0}{\omega_1}$$

$$X_{20} = \frac{X_{10}}{2}. \tag{A3}$$

In order to determine X_{10} and X_{20}, it is necessary to evaluate the static charge q_0, which depends on the bias condition of the diode and, hence, on the solution of (9).

B. Tripler Case

Following the same technique as for the doubler case, the maximum efficiency requires

$$\left(\frac{R_L'}{R_3} - 1 \right) \left(\frac{R_L'}{R_3} + 1 \right)^2 = \frac{m^2}{2\omega_1^4 R_1 R_2 R_3} P_{av} = k_3$$

$$\frac{R_g'}{R_1} = \frac{R_L'}{R_3} + 1$$

$$\psi_0 = \pi. \tag{A4}$$

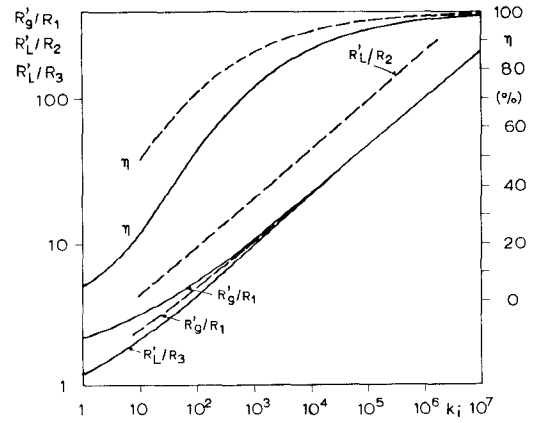

Fig. 12. Maximum efficiency and corresponding resistance values versus k_i; ---- doubler ($i=2$) and —— tripler ($i=3$).

Then

$$\cos^2\varphi_0=\frac{4}{9}\frac{R_1}{R_3}\frac{\dfrac{R'_L}{R_3}}{1+\dfrac{R'_L}{R_3}}\frac{\left[1+\dfrac{3}{2}k_3^{-1}\left(1+\dfrac{R'_L}{R_3}\right)^2\right]^2}{1+k_3^{-1}\left(1+\dfrac{R'_L}{R_3}\right)^2}\leqslant 1 \tag{A5}$$

and

$$\begin{aligned} X_{10}&=\frac{m}{\omega_1}(q_{20}\sin\varphi_0-2q_0)\\ X_{20}&=\frac{m}{2\omega_1}\left(\frac{q_{10}^2}{2q_{20}}\sin\varphi_0-2q_0\right)\\ X_{30}&=-\frac{m}{3\omega_1}2q_0. \end{aligned} \tag{A6}$$

The value of q_0 is obtained by numerically solving (9). It may be remarked that (A5) gives two values for φ_0, which are symmetrical about π. This means that two tuning conditions are possible, with the same value for maximum η.

The results of this Appendix are summarized in Fig. 12 which shows maximum efficiency and corresponding resistance values versus the parameter k_i ($i=2$ or 3 for a doubler or a tripler, respectively).

References

[1] E. Bava, G. P. Bava, A. De Marchi, and A. Godone, "Measurement of static AM–PM conversion in frequency multipliers," *IEEE Trans. Instrum. Meas.*, vol. IM-26, pp. 33–38, Mar. 1977.

[2] J. O. Scanlan, "Analysis of varactor harmonic generators," in *Advances in Microwaves*, vol. 2, Leo Young, Ed. New York: Academic Press, 1967, pp. 165–236.

[3] P. Penfield and R. P. Rafuse, *Varactor Applications*. Cambridge, MA: M.I.T. Press, 1962.

[4] K. Kurokawa, *An Introduction to the Theory of Microwave Circuits*. New York: Academic Press, 1969, p. 383.

[5] T. C. Leonard, "Prediction of power and efficiency of frequency doublers using varactors exhibiting a general nonlinearity," *Proc. IEEE*, vol. 51, pp. 1135–1139, Aug. 1963.

[6] C. C. H. Tang, "An exact analysis of varactor frequency multipliers," *IEEE Trans. Microwave Theory Tech.*, vol. MTT-14, pp. 210–212, Apr. 1966.

[7] G. B. Stracca, "Generazione di armoniche con diodi varactor," *Alta Frequenza*, vol. 31, pp. 134–149, Mar. 1962.

[8] ——, "Osservazioni sul progetto dei moltiplicatori di frequenza a varactor," *Alta Frequenza*, vol. 40, pp. 10–27, Jan. 1971.

[9] C. Dragone, "Phase and amplitude modulation in high efficiency varactor frequency multipliers of order $N=2^n$-stability and noise," *Bell Syst. Tech. J.*, vol. 46, pp. 797–834, Apr. 1967.

[10] V. Biro, "AM–PM conversion noise of abrupt-junction varactor frequency doublers," in *Proc. 3rd Colloquium on Microwave Communication*. Budapest: Akademiai Kiado, 1968, pp. 703–711.

[11] H. Groll and W. Berghofer, "Zur Instabilität von Varaktor-Vervielfachern," *Nachrichtentechnische Zeitschrift*, vol. 21, pp. 449–452, Aug. 1968.

[12] A. I. Grayzel, "The bandwidth of the abrupt-junction frequency doubler," *IEEE Trans. Circuit Theory*, vol. CT-13, pp. 52–58, Mar. 1966.

[13] J. O. Scanlan and P. J. R. Laybourn, "Bandwidth in varactor harmonic generators," *Proc. Inst. Elec. Eng.*, vol. 114, pp. 887–893, July 1967.